Thermal resistance measurement of edge-emitting semiconductor lasers using spontaneous emission spectra

© A.S. Payusov[1], A.A. Beckman[1], G.O. Kornyshov[2], Yu.M. Shernyakov[1], M.V. Maximov[2], N.Yu. Gordeev[1]

[1] Ioffe Institute,
194021 St. Petersburg, Russia
[2] Alferov University
194021 St. Petersburg, Russia

E-mail: plusov@mail.ioffe.ru

Received December 2, 2022
Revised December 8, 2022
Accepted December 8, 2022

An improved technique for thermal resistance measurement of edge-emitting diode lasers using spontaneous emission spectra, collected through the opening in the *n*-contact within the range of operating currents, has been proposed. The advantage of the proposed technique is that systematic errors typical for measurements based on lasing spectra are excluded. The accuracy of the method was verified by measuring the dependence of the thermal resistance on the cavity length for diode lasers with 100 μm strip width. Obtained results are in good agreement with the model, and the minimum measurement error was ± 0.1 K/W. The proposed technique can be used in metrological support of fabrication process of semiconductor lasers.

Keywords: laser diode, thermal resistance, spontaneous emission.

DOI: 10.21883/SC.2022.12.55152.4409

1. Introduction

Overheating of a crystal is one of the fundamental constraints limiting the efficiency and maximum power of edge-emitting semiconductor lasers. The thermal power density of modern high-power laser diodes at the maximum pump currents exceeds 10^2 W/mm^3, thus necessitating the use of active cooling systems. However, the active region overheating in modern diode lasers may reach 60–70 K [1] even when highly efficient heatsinks are used. An increase in temperature induces changes in the band gap width and the refraction index of materials forming a laser heterostructure. The carrier escape rate from the active region also increases, thus reducing the internal quantum efficiency [2]. In addition, the carrier density in the waveguide layer grows, and internal optical losses associated with free-carrier absorption increase accordingly [3]. Thus, overheating of devices exerts a negative influence on all the major parameters of lasers: the lasing wavelength, the threshold current density, the differential efficiency, and optical losses.

In order to diminish the overheating one need to increase the efficiency of current-light conversion, which depends on the internal quantum efficiency; internal optical losses; and the series resistance of a laser heterostructure, contact layers, and a metallization layer. At the same time, efficient heat transfer from the active region of a laser diode to the the cooler must be established. The key parameter of heat removal efficiency is the thermal resistance that is given by

$$R_T = \frac{\Delta T}{\Delta P_{\text{diss}}}, \tag{1}$$

where ΔT is the active region overheating and ΔP_{diss} is the dissipated thermal power, and characterizes the area where a temperature difference was measured. In a similar way to an electric circuit, one may construct a circuit for heat flow consisting of thermal resistances and capacitances. Since these capacitances may be neglected in continuous wave (CW) operation, the simplest thermal circuit characterizing a laser diode consists of thermal resistances, each of which corresponds to a specific structural element (laser heterostructure, solder heatsink, etc.), connected in series.

It follows from definition (1) that the thermal resistance can not be measured directly. The active region overheating of high-power laser diodes is often determined by measuring the long wavelength shift of the laser line [4], and the thermal resistance is calculated as

$$R_T = \frac{\partial\lambda/\partial P_{\text{diss}}}{\partial\lambda/\partial t} = \frac{\lambda'_P}{\lambda'_T}, \tag{2}$$

where λ'_P and λ'_T are the rates of the lasing wavelength shift with increasing dissipated power and temperature, respectively. The temperature dependence of the lasing wavelength is commonly measured in the pulsed mode to avoid unwanted self heating. The dissipated thermal power may be calculated using the following formula:

$$P_{\text{diss}} = I \cdot U - P_{\text{out}}, \tag{3}$$

where P_{out} is the output optical power, I is the laser pump current, and U is the voltage drop across the laser diode. The thermal resistance measured this way for the best laser diodes with a stripe width of 100 μm and 4 mm in length mounted on heatsink falls within the 1.5–2.5 K/W range [1,5], with data on measurement error is often being omitted. However, usage of the lasing line as an indicator of temperature of the active region may be a source of a

considerable systematic error. The temperature shift of the lasing line is governed not only by changes in the band gap width of the material of the active region, but also by variations of the modal gain and loss spectra. This is manifested, e.g., in a weak temperature dependence of the lasing wavelength of quantum dot lasers [6]. Depending on the waveguide design, the shift rate may be up to two times lower than the one corresponding to quantum well lasers. The lasing line of high-power semiconductor lasers in CW operation at high current densities often shifts to shorter wavelength range [7]. The thermal resistance calculated in accordance with formula (2) may thus depend strongly on the pump current [8] and even be negative [9]. Therefore, one needs to improve the considered method by excluding the possible systematic error sources.

In the present study, we propose to use spontaneous emission spectra of the active region measured through an opening in the *n*-contact at pump currents corresponding to a high output power to determine accurately the thermal resistance of edge-emitting laser diodes.

2. Measurement technique of spontaneous emission spectra

All the experimental results reported below were obtained using broad area laser diodes with a stripe contact width of 100 μm, which were examined in [10] (and denoted as NWG). Lasers were mounted p-side down onto copper heatsink with indium solder. Openings in the metal of n-contact were made afterward for measurements of spontaneous emission, which propagated along the normal to the heterostructure layers. Spontaneous emission was collected with an optical fiber 100 μm in diameter. Measurements of spectra in CW regime were performed using the lock-in technique, for which the laser emission was modulated using optical chopper. Pulsed measurements were carried out under pumping by a current exceeding the threshold one by a factor of 1.5–2, the pulse duration was 350 ns, and the frequency was 10 kHz). The signal was detected by an InGaAs receiver with a bandwidth of 150 MHz and a gated integrator and boxcar averager. The duration of gating pulses were set to be 50–100 ns shorter than pump ones in order to exclude the influence of pulse edges on measurements. Averaging over 10^3 pulses was performed to enhance the signal-to-noise ratio. A temperature (t°_{hs}) of the laser heatsink was maintained constant during the course of measurements using a Peltier based temperature controller. A small-sized resistive temperature detector was positioned on the heatsink surface in the close proximity of the laser crystal. The sensor position remained the same in all measurements. The optical power in the CW regime was measured with a bolometer with a photosensitive area 25 mm in diameter. The voltage drop across the laser was measured with a five-digit digital voltmeter. Since spontaneous emission was collected from the *n*-contact side, the optical power was measured simultaneously with the spontaneous emission spectra throughout the entire experiment. This allowed us to determine the moment of onset and the nature of degradation of the examined devices accurately. Lasers with a cavity length of 4 mm demonstrated maximum optical power in excess of 7 W at a pump current of 11 A, which was limited by catastrophic optical degradation.

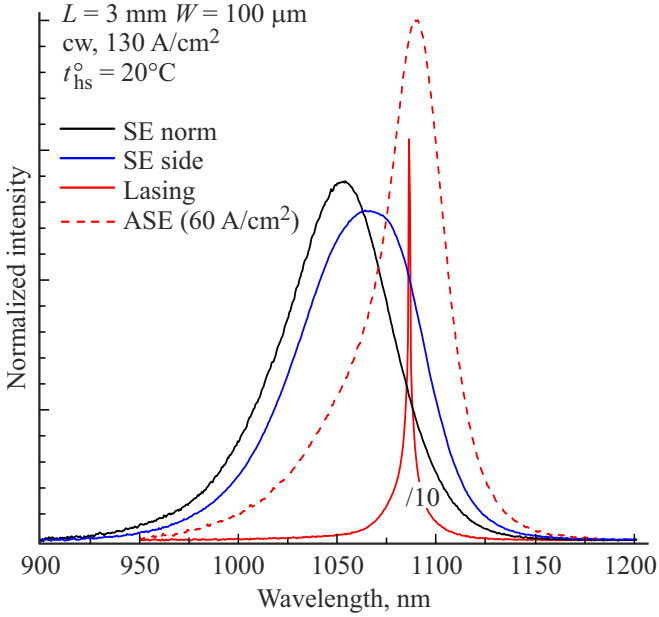

Figure 1. Emission spectra (normalized to a unit area) of the laser diode measured in the CW regime at the lasing threshold from the output mirror (lasing), from the side face (SE side), and normally to the heterostructure layers (SE norm). The ASE spectrum measured at a current equal to the half threshold current is represented by the red dashed curve. (A color version of the figure is provided in the online version of the paper).

Spontaneous emission may be measured from different facets of the laser crystal (Fig. 1). Emission entrapped in one of the waveguide modes and amplified via interaction with the active region in multiple reflections (amplified spontaneous emission, ASE) propagates along the cavity axis. At currents above threshold, the lasing line is superimposed with ASE. A mixture of amplified spontaneous emission and spontaneous emission propagating freely within the crystal is output though the side face. Amplified spontaneous emission is confined to the waveguide layer and cannot propagate normally to the laser heterostructure layers. Therefore, the determination of temperature of the active region based on spontaneous emission spectra measured normally allows one to exclude systematic errors induced by the temperature and current dependences of the modal gain and losses. In what follows, we use the term „spontaneous emission“ without specifying that this emission is measured along a normal to the heterostructure layers.

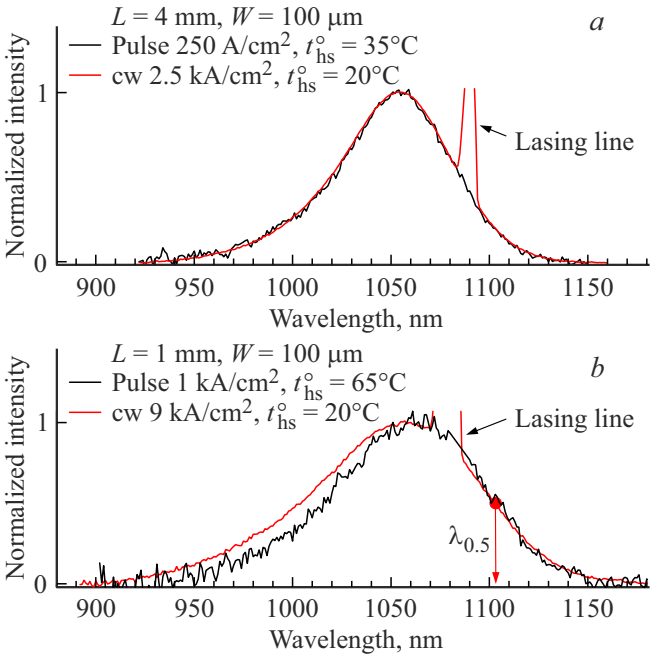

Figure 2. Spontaneous emission spectra measured in CW (red curves) and pulsed (black curves) regimes for lasers with a cavity length of ~ 4 mm (a) and ~ 1 mm (b).

3. Thermal resistance measurement

The spectrum of density of states of the active region, the carrier density in the active region, and temperature affect the position of the maximum and the shape of the spontaneous emission spectrum. An increase of the carrier density leads to a short wavelength shift of the maximum of spontaneous emission spectra due to Moss-Burstein effect. The temperature dependence is induced both by changes in the band gap width and the filling of high-energy states at higher temperatures. The band gap shrink at higher temperatures results in a long wavelength shift, and an increase of the population of high-energy states leads to the change of the short wavelength tail of the spontaneous emission spectrum. At the same time, an increase of the carrier density in the active region does not affect the long wavelength tail of the spontaneous emission spectrum. Therefore, it could be used for accurate temperature measurements.

When the threshold condition is satisfied, the carrier density in high-power laser diodes depends only weakly on the pump current, the active region overheating is limited to 20 K at current densities up to $2-3$ kA/cm^2, and the shape of the spontaneous emission spectrum remains almost unchanged (Fig. 2, a). A shorter laser (Fig. 2, b) operates at a current density of 9 kA/cm2, and a 45 K overheating of the active region does increase internal optical losses. A higher optical gain is needed to maintain lasing, and the carrier density in the active region increases. Hence, the shape of the spontaneous emission spectrum measured in the CW regime deviates from the shape of the spectrum measured in the pulsed mode at an elevated temperature. Wavelength λ_0 of the maximum then becomes an inaccurate indicator of the active region temperature, since the Burstein–Moss shift compensates partially the long wavelength shift induced by heating. However, the shape of long wavelength tail of spectra measured in CW and pulsed regimes match, and one may determine overheating by monitoring wavelength $\lambda_{0.5}$ of the long wavelength tail at half maximum (see Fig. 2, b). Having measured approximately 50 laser diodes with different designs of the waveguide [12] and the active region [9], we observed no variation in the shape of long wavelength tail of spontaneous emission spectra at the maximum pump currents. Note also that laser diodes with a record-high output power presently operate at current densities around 10 kA/cm^2 [1,5]. Thus, the proposed method allows one to measure the thermal resistance in the required range of pump currents. Having measured the dependences of the wavelength of the spontaneous emission maximum on temperature in the pulsed regime and wavelength $\lambda_{0.5}$ in CW regime, one may use formula (2) to calculate the thermal resistance.

In order to measure wavelengths λ_0 and $\lambda_{0.5}$ accurately and determine the measurement error, we performed approximation of spontaneous emission spectra using the method of least squares and the following function:

$$f(\Lambda) = \frac{1}{\Lambda_A^6 + \Lambda_A^4 + \Lambda_A^2 + 1} + \frac{1}{\Lambda_B^6 + \Lambda_B^4 + \Lambda_B^2 + 1}, \quad (4)$$

where

$$\Lambda_A = \left(\frac{2(\lambda - \lambda_A)}{\omega_A}\right), \quad \Lambda_B = \left(\frac{2(\lambda - \lambda_B)}{\omega_B}\right). \quad (5)$$

An example of this approximation and the physical meaning of parameters in formulae (4) and (5) are presented in Fig. 3. The least squares approximation provides a standard

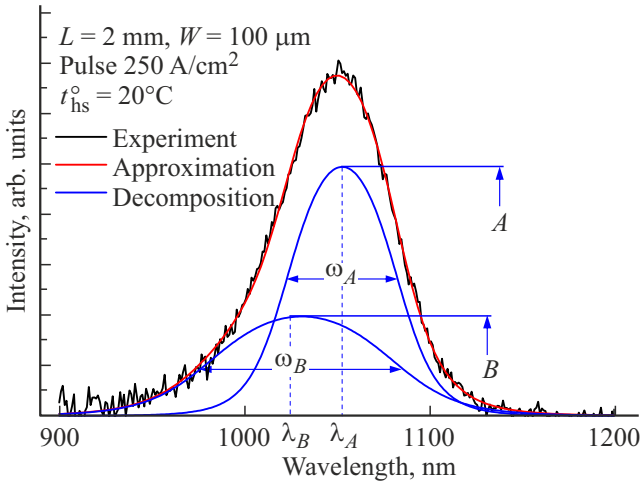

Figure 3. Approximation of the spontaneous emission spectrum and its decomposition into two peaks with amplitudes A and B, wavelengths λ_A and λ_B, and widths ω_A and ω_B.

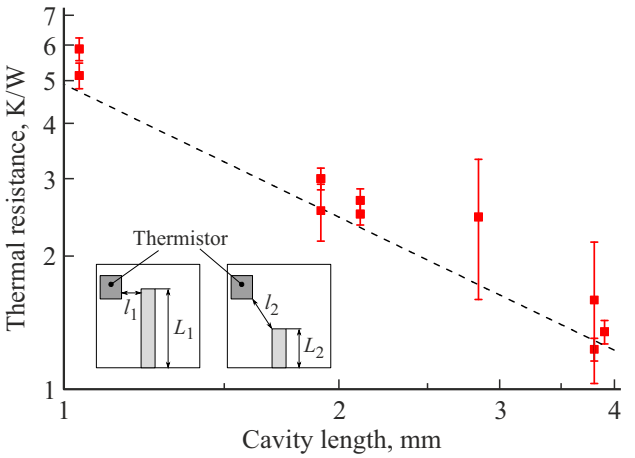

Figure 4. Experimental dependence of the thermal resistance on the laser cavity length. The dashed curve corresponds to a specific thermal resistance of 4.9 mm · K/W. Error bars correspond denote the standard error. Heatsinks with mounted lasers of different lengths (L_1 and L_2) are shown schematically in the inset; l_1 and l_2 are the corresponding distances between the laser diode and the temperature sensor.

error for each parameter. It is demonstrated below that the values and standard error of wavelengths λ_0 and $\lambda_{0.5}$ could be expressed in terms of approximation parameters and their standard errors. We have also approximated the experimental spectra by a sum of two Gaussian curves, and the sum of mean-square deviations differed insignificantly from the result of approximation with expression (4). At the same time, polynomials are much more convenient, since they may be treated as numbers in programming languages (GNU Octave, Matlab, etc.). The validity of the proposed method was estimated by measuring a series of samples with different cavity lengths. In the simplest model, the thermal resistance of laser diodes with the same width of a stripe contact is inversely proportional to laser cavity length L:

$$R_T = \frac{\rho_T}{L}, \tag{6}$$

where ρ_T is the specific thermal resistance. In a double logarithmic scale, dependence R_T specified by formula (6) is a straight line with a negative unity slope. The measured dependence in a logarithmic scale fits well with the line corresponding to a specific thermal resistance of 4.9 mm · K/W (Fig. 4). A slight increase in the thermal resistance of lasers with a cavity length of 1 mm relative to the specific thermal resistance line originates from the specific positioning of the temperature sensor (see the inset of Fig. 4). When short laser diodes are being mounted, the distance between the sensor and the laser crystal increases slightly, and an additional thermal resistance, which adds up to the overall thermal resistance of short lasers, is introduced into the thermal circuit. The minimum standard error of our measurement was ±0.1 K/W.

4. Calculation of the measurement error

The random error is commonly characterized using standard error. The error of thermal resistance measurements may be calculated using the following well-known formula for the prorogation of error:

$$\Delta f(x_1 \dots x_n)^2 = \sum_{i=1}^{n} \left(\frac{\partial f}{\partial x_i} \cdot \Delta x_i \right)^2, \tag{7}$$

where Δf is the standard error of the measured value, $x_1 \dots x_n$ are parameters on which this value depends, and $\Delta x_1 \dots \Delta x_n$ are their standard errors. Applying formula (7) to expression (2), we obtain

$$\Delta R_T = \sqrt{\left(\frac{1}{\lambda'_T} \Delta\lambda'_P \right)^2 + \left(\frac{\lambda'_P}{(\lambda'_T)^2} \Delta\lambda'_T \right)^2}, \tag{8}$$

where λ'_P and λ'_T are errors for the slopes of current and temperature dependences of spontaneous emission. They may be determined via linear approximation of the corresponding dependencies using least square method and introducing errors $\Delta\lambda_0$ and $\Delta\lambda_{0.5}$ as weight coefficients. Therefore, in order to determine errors λ'_P and λ'_T, one needs to know $\Delta\lambda_0$ and $\Delta\lambda_{0.5}$. Error $\Delta\lambda'_T$ may be reduced by averaging the measurements of different devices fabricated from the same heterostructure. Since λ_T measurements are performed in the pulsed mode at a low current density, variations originating from imperfections of mounting and post-growth processing have almost no effect on the measurement results. Random error $\Delta\lambda'_P$ may be reduced only by increasing the sample size. However, an irreversible degradation of a laser diode may occur at high CW current densities. Therefore, the number of measurements of one laser should not be too high.

First, one needs to calculate λ_0 and $\lambda_{0.5}$ using the values of fitting parameters (Fig. 3). Let us use the wavelength of the maximum of curve (4) as a nominal λ_0 value. It is evident that it lies between λ_A and λ_B (Fig. 3). Let us introduce the following notation:

$$\delta = (\lambda_A - \lambda_B), \quad k = \frac{B}{A}, \quad m = \frac{\omega_B}{\omega_A} \tag{9}$$

and a new variable:

$$t = 2\left(\lambda - \lambda_A + \frac{\delta}{2}\right) = 2\left(\lambda - \lambda_B - \frac{\delta}{2}\right). \tag{10}$$

Following the substitution of variables in (5) with notation (9) taken into account, the polynomials in denominators of the first and the second terms in (4) transform into

$$P_6(t) = \left(\frac{t-\delta}{\omega_A} \right)^6 + \left(\frac{t-\delta}{\omega_A} \right)^4 + \left(\frac{t-\delta}{\omega_A} \right)^2 + 1, \tag{11}$$

$$Q_6(t) = \left(\frac{t+\delta}{m\omega_A} \right)^6 + \left(\frac{t+\delta}{m\omega_A} \right)^4 + \left(\frac{t+\delta}{m\omega_A} \right)^2 + 1. \tag{12}$$

Next, we perform the substitution of variables in $P_6(t)$:

$$r = \left(\frac{t-\delta}{\omega_A}\right), \quad r_0 = -\frac{\delta}{\omega_A}, \quad (r - r_0) = \frac{t}{\omega_A} \tag{13}$$

and apply the Taylor series for polynomials. $P_6(t)$ then takes the form

$$P_6\left(\frac{t}{\omega_A}\right) = \sum_{n=0}^{6} a_n \cdot \left(\frac{t}{\omega_A}\right)^n. \tag{14}$$

$Q_6(t)$ is processed in a similar way:

$$r' = \left(\frac{t+\delta}{m\omega_A}\right); \; r'_0 = \left(\frac{\delta}{m\omega_A}\right); \; (r' - r'_0) = \frac{t}{m\omega_A}, \tag{15}$$

$$Q_6\left(\frac{t}{\omega_A}\right) = \sum_{n=0}^{6} \frac{b_n}{(m)^n} \cdot \left(\frac{t}{\omega_A}\right)^n. \tag{16}$$

Thus, we transformed expression (4) to the form

$$f\left(\frac{t}{\omega_A}\right) = \frac{A}{P_6(t/\omega_A)} + \frac{kA}{Q_6(t/\omega_A)}. \tag{17}$$

The polynomials in (17) are now functions of the same argument. We find the maximum of function (17) by equating its first derivative to zero:

$$P'_6\left(\frac{t}{\omega_A}\right)\left(Q_6\left(\frac{t}{\omega_A}\right)\right)^2 + k\,Q'_6\left(\frac{t}{\omega_A}\right)\left(P_6\left(\frac{t}{\omega_A}\right)\right)^2 = 0. \tag{18}$$

Expression (18) is a polynomial of degree 12. It has one real-valued root (t_0). Having found it, we determine the position of maximum (λ_0) with the use of (10). We determine the value of function $f_{\max}$ at λ_0 by inserting t_0 into (17). The nominal value of $\lambda_{0.5}$ is obtained by solving equation

$$\frac{f_{\max}}{2} = \frac{A}{P_6(t_{0.5}/\omega_A)} + \frac{kA}{Q_6(t_{0.5}/\omega_A)} \tag{19}$$

for $t_{0.5}$.

We find error $\Delta\lambda_0$ using formula (7) and expression (10):

$$\Delta\lambda_0^2 = \left(\frac{\Delta\lambda_A}{2}\right)^2 + \left(\frac{\Delta\lambda_B}{2}\right)^2 + \left(\frac{t_0}{2}\Delta\omega_A\right)^2 + \left(\frac{\omega_A}{2}\Delta t_0\right)^2. \tag{20}$$

Errors $\Delta\lambda_A$, $\Delta\lambda_B$, and $\Delta\omega_A$ resulted from approximation, and the unknown Δt_0 error may be determined using (7) once again, since

$$t_0 = f\left(k, m, \frac{\delta}{\omega_A}\right). \tag{21}$$

Partial derivatives, which emerge when (7) is applied to (21), are easy to calculate numerically using expression (17). Thus, we have expressed error $\Delta\lambda_0$ in terms of errors of fitting parameters.

In order to find errors $\Delta\lambda_{0.5}$, one needs to know $\Delta f_{\max}$, which may be determined using the relation

$$f_{\max} = f\left(A, k, m, \frac{\delta}{\omega_A}\right). \tag{22}$$

Error $\Delta\lambda_{0.5}$ may be determined using (4) and relation [13]

$$\Delta\lambda_0 = f'(\lambda_0)\Delta f_{\max}. \tag{23}$$

When calculating λ'_P and λ'_T, one also needs to take the errors of measurement instruments into account. In our case, the measurement errors were equal to the systematic error of our instruments, which is typically given in the instrument certificate. We summed up systematic γ and random $\Delta\lambda$ errors in the following way [13]:

$$\sum = \gamma + 2\Delta x^2. \tag{24}$$

Thus, we have demonstrated how the values of λ_0 and $\lambda_{0.5}$ may be derived from fitting parameters. Having plotted the dependencies of the wavelength on temperature and the dissipated power, we determined wavelength shift rates λ'_P, λ'_T and their standard errors and then used formula (8) to calculate the thermal resistance and error ΔR_T.

5. Conclusion

An improved technique for measurement of the thermal resistance of edge-emitting laser diodes using spontaneous emission spectra measured through an opening in the *n*-contact at currents corresponding to a high output power was proposed, and the measurement error was analyzed. The advantage of the method is that it excludes systematic errors, which are typical for measurements of the thermal resistance based on lasing spectra. The accuracy of the improved technique was verified experimentally with measurements of the dependence of thermal resistance of laser diodes with 100 μm stripe width on the cavity length. The minimum error was ± 0.1 K/W. The proposed technique may be used to provide metrological support for production of semiconductor lasers.

Acknowledgments

A.S. Payusov would like to thank V.P. Evtikhiev, a senior research fellow of the Ioffe Institute, for fruitful discussions.

Funding

This work was supported by the Russian Science Foundation (project No. 22-22-00557), https://rscf.ru/project/22-22-00557/

Conflict of interest

The authors declare that they have no conflict of interest.

References

[1] V. Gapontsev, N. Moshegov, I. Berezin, A. Komissarov, P. Trubenko, D. Miftakhutdinov, I. Berishev, V. Chuyanov, O. Raisky, A. Ovtchinnikov. SPIE LASE (February 22, 2017, San Francisco, California, USA) p. 1008604.

[2] B.S. Ryvkin, E.A. Avrutin. J. Appl. Phys., **97**, 113106 (2005).
[3] D.A. Veselov, Y.K. Bobretsova, A.A. Klimov, K.V. Bakhvalov, S.O. Slipchenko, N.A. Pikhtin. Semicond. Sci. Technol., **36**, 115005 (2021).
[4] T.W. Hänsch, G.T. Kamiya, T.F. Krausz, G.B. Monemar, L.M. Ohtsu, T.H. Venghaus, B.H. Weber, B.H. Weinfurter. *High Power Diode Lasers* (Springer New York, N.Y., 2007).
[5] P. Crump, H. Wenzel, G. Erbert, G. Tränkle. SPIE LASE (8 February, 2012, San Francisco, California, USA) p. 82410U.
[6] F. Klopf, S. Deubert, J.P. Reithmaier, A. Forchel. Appl. Phys. Lett., **81**, 217 (2002).
[7] N.K. Dutta, J. Jaques, A.B. Piccirilli. Electron. Lett., **38**, 513 (2002).
[8] V.V Bezotosnyi, O.N. Krokhin, V.A. Oleshchenko, V.F. Pevtsov, Y.M. Popov, E.A. Cheshev. Quant. Electron., **46**, 679 (2016).
[9] A.S. Payusov, N.Y. Gordeev, A.A. Serin, M.M. Kulagina, N.A. Kalyuzhnyy, S.A. Mintairov, M.V. Maximov, A.E. Zhukov. Semiconductors, **52**, 1901 (2018).
[10] Yu.M. Shernyakov, N.Yu. Gordeev, A.S. Payusov, A.A. Serin, G.O. Kornyshov, A.M. Nadtochiy, M.M. Kulagina, S.A. Mintairov, N.A. Kalyuzhnyy, M.V. Maximov, A.E. Zhukov. Semiconductors, **55**, 333 (2021).
[11] E. Burstein. Phys. Rev., **93**, 632 (1954).
[12] A.A. Beckman, A.S. Payusov, G.O. Kornyshov, Y.M. Shernyakov, S.A. Mintairov, N.A. Kalyuzhnyy, M.M. Kulagina, M.V. Maximov, N.Y. Gordeev. *2022 Int. Conf. Laser Opt.* (June 20–24, 2022, Saint Petersburg) p. 1.
[13] A.N. Zaidel'. *Oshibki izmerenii fizicheskikh velichin* (L., Nauka, 1974) (in Russian).